JOURNAL OF Materials CHEMISTRY

Preparation and characterization of $CuO–ZrO_2$ nanopowders

Yanqin Wang and Rachel A. Caruso*

Max Planck Institute of Colloids and Interfaces, D-14424 Potsdam, Germany.
E-mail: rcaruso@mpikg-golm.mpg.de

Received 27th November 2001, Accepted 5th March 2002
First published as an Advance Article on the web 3rd April 2002

Nanosized copper oxide–zirconia particles containing 10–30 mol% of copper were prepared by using a precipitation technique in aqueous tetramethylammonium hydroxide solutions. Two methods, *in situ* (INS) and step-by-step (SBS), which differed in the time when the copper salt was introduced to the synthesis procedure, were used, and this allowed a comparison of the properties of the final powders produced using the two modes of preparation. The surface areas and phase compositions were different for the samples prepared from the two different methods after calcination at 500 °C. A surface area of 168 $m^2\ g^{-1}$ was obtained for the sample prepared with the SBS method and 121 $m^2\ g^{-1}$ for the INS method, both contain 30 mol% copper. Tetragonal ZrO_2 was observed from X-ray diffraction patterns for all samples prepared with the SBS method, however, no separate phase of copper or copper oxide was observed. It is proposed that all of the copper is finely distributed on the surface of the ZrO_2 particles with the SBS method. For the samples prepared from the INS method, tetragonal ZrO_2 was obtained at a low copper content and the peaks indexed to tetragonal ZrO_2 shifted to higher angle with the increase of copper content, indicating copper ions being incorporated into the lattice. An amorphous compound was obtained at high copper content (30 mol%). The phase change with the calcination temperature was also investigated for the INS sample containing 30 mol% copper. The studies show that tetragonal ZrO_2 and copper oxide were present after calcination at 400 °C, and tetragonal ZrO_2 with a small amount of monoclinic ZrO_2, as well as copper oxide, formed after calcination at 700 °C. However, after heating at 500 °C, amorphous compounds were obtained, suggesting that 500 °C could be a phase transition point. The incorporation of copper in the ZrO_2 lattice resulted in a loss of order in the ZrO_2 structure when calcined at 500 °C, with a further increase in the calcination temperature leading to the phase change.

Introduction

Supported copper catalysts have high catalytic activities in, for example, the synthesis of methanol,[1–5] methanol–steam reforming,[6,7] oxidation of carbon monoxide,[8–11] and NO[12] and N_2O[13] decomposition. Hence numerous studies altering the type of copper precursor and varying the support material have been conducted to control the formation of such materials and compare the catalytic activities. Zirconia supports are of particular interest as they can possess relatively high surface areas, they are mechanically and thermally stable, are solids with adsorbent properties, as well as being catalysts themselves. Zirconia supported copper catalysts have been shown to have high activities and selectivities for NO-CO reactions at low temperature,[8,11] to be active in the decomposition of N_2O,[13] and are active and selective for methanol synthesis from carbon dioxide.[2,14–16]

Copper–zirconia catalysts can be prepared using a variety of wet-chemical methods including sol–gel,[2] impregnation,[17] and co-precipitation.[15,17,18] The structural properties, and hence catalytic activities of the materials obtained using these techniques vary substantially. Using the sol–gel synthesis the final copper–zirconia particles are interdispersed, whereas impregnation techniques generally result in copper nanoparticle formation on the surface of the preformed zirconia material. Co-precipitation methods, like the sol–gel synthesis, give more evenly dispersed copper and zirconia particles, with the possibility of copper ion incorporation within the zirconia lattice. Overall the copper particles are distributed more evenly with sol–gel and co-precipitation methods, therefore giving larger copper surface areas, and there is a higher degree of copper–zirconia interfacial contact. Both of these properties (the surface area of the metal and interfacial contact area between the copper and zirconia) have been found to be crucial factors for catalytic performance.[17] Wambach *et al.*[19] have recently reviewed the preparation of metal–zirconia catalysts along with their structural and chemical characteristics, and the catalytic properties for carbon dioxide hydrogenation.

This paper reports the preparation of copper oxide–zirconia powders with high surface area and different contents of copper, and compares the morphological properties of the materials obtained from the two selected syntheses. As particles decrease in size, it is known that the number of atoms in the surface layer increases compared to the number of atoms in the bulk. Therefore, a method to potentially enhance the catalytic activity of a material would be to form metal particles on the surface of a nanosized support, thereby resulting in high metal loading quantities, giving an increase in the surface area of the metal and forming a larger area of interfacial contact overall. The copper–zirconia nanopowders were prepared by a tetramethylammonium hydroxide (TMAOH) precipitation method from aqueous copper(II)–zirconium(IV) precursor solutions through either *in situ* (one-stage) or step-by-step (two-stage) preparation. TMAOH was chosen as the precipitant for a number of reasons: in terms of the copper it was chosen because TMA^+ ions are quaternary ions that cannot form complexes with Cu^{2+}, while other amine ions can form stable complexes with Cu^{2+}.[20] Additionally, tetraalkylammonium salts are commonly used to stabilize metal colloids because the cations adsorb on the surface of the metal particles.[21–23] For the support material it was believed that nanoparticles of zirconia could also be formed in a controlled manner as tetraalkylammonium hydroxide has recently been used to prepare titanium dioxide[24] and yttrium oxide[25] nanocrystals with good control over different morphologies, giving narrow size distributions.

 DOI: 10.1039/b110844a

Experimental procedure

Materials

The zirconia precursor, zirconium propylate [$Zr(OPr)_4$, 70% in propanol], copper salt, copper nitrate [$Cu(NO_3)_2{\cdot}2.5H_2O$], and the precipitant, tetramethylammonium hydroxide [$(CH_3)_4N{\cdot}OH$, 25% in methanol, TMAOH] were all purchased from Aldrich and used without further purification. Deionised water was used as the solvent.

Preparation of $CuO–ZrO_2$ powders

Two methods were used to prepare these samples. One was the *in situ* (INS) preparation: in this method, 5 mL $Zr(OPr)_4$ was added dropwise to an aqueous solution of TMAOH (2.5 mmol, 43–25 mL), and stirred for 1 h. Then a calculated amount of a 0.5 M $Cu(NO_3)_2$ aqueous solution (2.2–25 mL) was added according to the molar ratio of copper to zirconium, making a final volume of 50 mL. The mixture was stirred for another 1 h at room temperature, and then heated at 80 °C for 20 h. The sample was collected by centrifugation, washed with water and then ethanol, dried overnight (60 °C), and finally calcined at 500 °C for 12 h under air (ramp 2 °C min^{-1}). The other method was the step-by-step (SBS) preparation: in this procedure, the aqueous solution of $Cu(NO_3)_2$ (0.5 M) was added after the aqueous TMAOH–zirconia precursor suspension had been heated at 80 °C for 20 h. Heating at 80 °C continued for another 6 h, and the following steps were kept identical to those used in the *in situ* method.

Note that the percent copper given refers to the content of copper relative to total copper and zirconium content in the synthesis solution.

Characterization

To obtain data on the crystal phase of the sample, X-ray powder diffraction (XRD) patterns were obtained using an Enraf-Nonius PDP-120 diffractometer, with Cu-Kα irradiation. Transmission electron microscopy (TEM) studies, to observe particle morphology and size, were carried out on a Zeiss EM 912 Omega electron microscope. The samples for TEM were prepared by dispersing the final powders in ethanol, which was placed on carbon-coated copper grids. The nitrogen adsorption and desorption isotherms at 77 K were measured using a Micromeritics instrument (Tristar 3000) after the samples were evacuated at 150 °C overnight. BET (Brunauer, Emmett and Teller) surface areas were calculated from the linear part of the BET plot. Thermogravimetric analysis (TGA) was carried out on a Netzsch TG 209 instrument to estimate the temperature for removal of organic materials.

Results and discussion

TMAOH has previously been used as a catalyst and stabilizer in the formation of titania[24] and yttrium oxide[25] nanoparticles. The addition of zirconium propylate to aqueous TMAOH solutions results in the hydrolysis and condensation of the zirconia precursor and thus the formation of a white precipitate. When copper nitrate was added to the suspension it becomes sky-blue in color and the as-prepared sample obtained after drying at 60 °C was also sky-blue. These as-prepared samples changed to a green color during calcination at 500 °C, except for the samples containing 50% copper, which were black–green.

Thermogravimetric analysis was performed to obtain information on the temperature at which the solvent and organic material was removed from the hybrid sample. Fig. 1 shows the TGA curves of the samples with 10% copper, prepared by using the INS and SBS methods (ramp 20 °C min^{-1}, O_2 atmosphere). The TGA curves of other samples containing higher contents of copper are similar to these two samples (data not shown). As a comparison, the TGA curve for a ZrO_2 material (0% Cu) is also shown in Fig. 1. It can be seen from this figure that the solvents and organic materials were all removed before 400 °C.

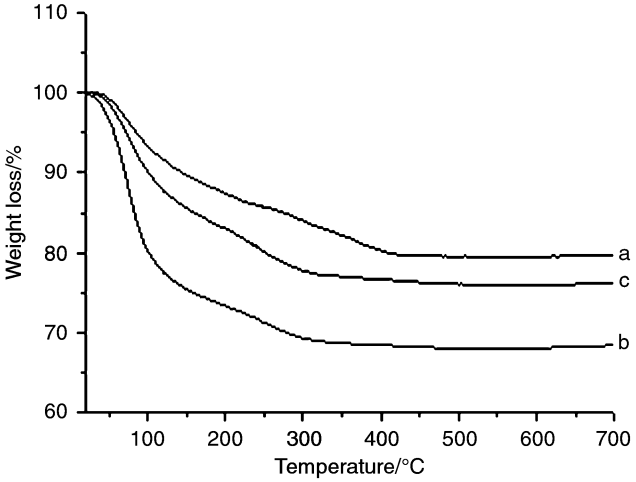

Fig. 1 TGA curves of a) ZrO_2 (0% Cu); b) $CuO–ZrO_2$ (10% copper), prepared by using the INS method; c) $CuO–ZrO_2$ (10% copper), prepared by using the SBS method. Experiments conducted under oxygen with a ramp rate of 20 °C min^{-1}.

Gas adsorption of the as-prepared and calcined samples allowed calculation of the BET specific surface area of the materials. These properties (along with the particle size obtained from X-ray data, which will be discussed later) for the samples obtained from both the INS and SBS preparation methods are given in Table 1. The surface area is seen initially to increase with the increase in copper content, with a maximum for 30% copper, and decrease for copper contents of 50%, for both synthesis methods. The increase of surface area with the increase of copper content (10–30%) is expected to be due to the contribution of the copper species, especially in the SBS preparation. The surface areas of the samples prepared with the SBS method are higher than those prepared with the INS method for the same content of copper. This difference in the surface area between the two methods could be explained after examination of the XRD data.

The differences between the samples prepared with the two different methods are apparent not only from the surface area data, but also from changes in phase composition. Figs. 2 and 3 show the XRD patterns of the samples from both methods calcined at 500 °C and Table 1 also shows the particle sizes of crystalline zirconia using the Scherrer equation[26] from the XRD patterns. The mean particle size obtained by using the INS method is higher than that obtained from the SBS method, hence the surface area in the case of the INS method is lower than the SBS method for samples containing the same copper content. The mean particle size changes slightly with increasing copper content, indicating that the presence of the copper species has little effect on the crystalline size of zirconia and the

Table 1 BET specific surface areas (SA) of both the INS and SBS samples [as-prepared and after calcination at 500 °C] from nitrogen adsorption data. Particle sizes, *d*, of crystalline zirconia [after calcination at 500 °C] calculated from XRD pattern

Cu content (mol %)	SA/m^2 g^{-1} as-prepared		SA/m^2 g^{-1} calcined		*d* /nm	
	INS	SBS	INS	SBS	INS	SBS
10	296	336	72	110	14	9
15	301	509	111	158	16	8
30	330	546	121	168		11
50	250	520	71	41		

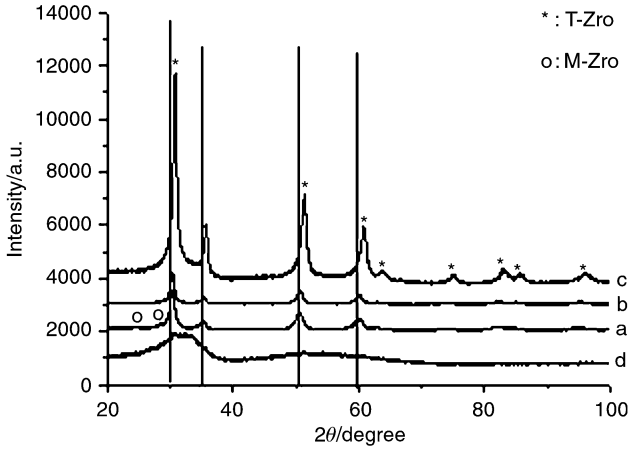

Fig. 2 XRD patterns of the samples obtained after calcination at 500 °C prepared by using the INS method and containing a) 0, b) 10, c) 15, and d) 30% copper. The abbreviations T-ZrO and M-ZrO signify tetragonal and monoclinic zirconia, respectively.

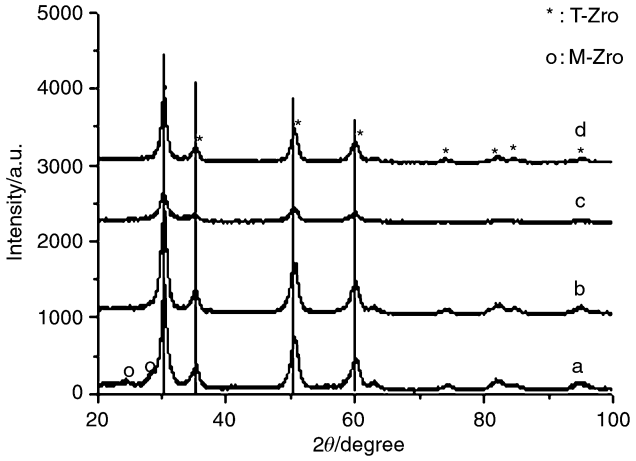

Fig. 3 XRD patterns of the samples obtained after calcination at 500 °C prepared by using the SBS method and containing a) 0, b) 10, c) 15, and d) 30% copper. The abbreviations T-ZrO and M-ZrO signify tetragonal and monoclinic zirconia, respectively.

increase in surface area with increasing copper content is due to contributions from the copper species. The XRD pattern of pure ZrO_2 prepared with the same method is also shown in Figs. 2a and 3a, for comparison. The tetragonal phase is dominant with a small amount of the monoclinic phase after calcination at 500 °C for the pure zirconia, which is different to the samples containing copper where only the tetragonal ZrO_2 was formed. Other studies have indicated that the addition of low contents (less than ~16 mol%) of aliovalent cations stabilizes the formation of the tetragonal phase.[27]

For the samples prepared with the INS method, the XRD patterns shown in Fig. 2 demonstrate that tetragonal ZrO_2 was formed when the content of copper was in the range of 10–15%. The peaks indexed to tetragonal ZrO_2 are seen to shift to higher angle with the increase of copper content, indicating Cu^{2+} ions are being incorporated into the zirconia lattice (*i.e.* they occupy the position of the Zr);[28] while an amorphous composite was formed when the content of copper reached 30%. The effect of the copper content on the phase of ZrO_2 was investigated at different calcination temperatures. Fig. 4 shows the XRD patterns of the copper oxide–zirconia materials (with 30% Cu) calcined at 400 (12 h calcination), 500 (12 h) and 700 °C (8 h). It can be seen that tetragonal ZrO_2 and CuO exist after calcination at 400 °C, whereas after heating at 700 °C the CuO still exists but the zirconia consists of the tetragonal phase with a small amount of monoclinic ZrO_2. From the existence of the

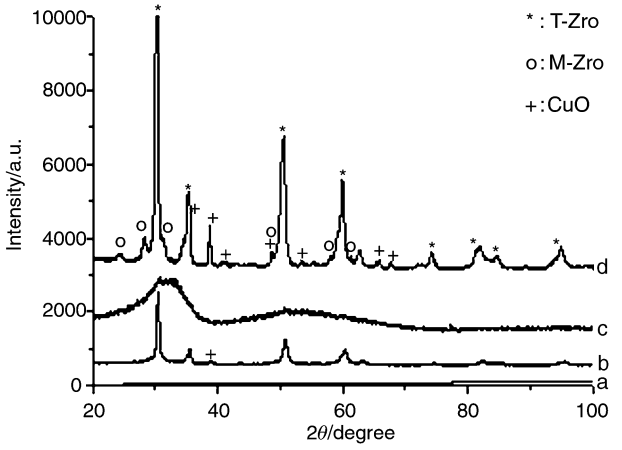

Fig. 4 XRD patterns of the samples containing 30% copper (INS method) calcined at different temperatures: a) 250 °C; b) 400 °C; c) 500 °C; and d) 700 °C. The abbreviations T-ZrO_2 and M-ZrO_2 signify tetragonal and monoclinic zirconia, respectively.

CuO peaks and the shift of peaks indexed to tetragonal ZrO_2, it is believed that most copper existed as a separate phase and a small amount was incorporated in the lattice. However, the crystalline structure was destroyed after heating at 500 °C; this could be attributed to the incorporation of Cu^{2+} ions in the lattice, which disrupted the structure. Hence, it is suggested that 500 °C could be a transition point and that phase change occurs above this temperature. The phase change of nanosized zirconia from tetragonal at low temperature to the mixture of tetragonal and monoclinic has been observed previously.[27]

For the samples prepared with the SBS method, XRD patterns (Fig. 3) demonstrate that tetragonal ZrO_2 was formed and no separate phase of copper or copper oxide was detected at all contents of copper. It is proposed that the copper species (ions and/or very small CuO clusters) are finely distributed on the surface of the ZrO_2 particles, which leads to the higher surface areas and the increase in surface area with increasing copper content up to 30%.

TEM images of the samples containing 30% copper obtained using the INS and SBS methods (not shown) indicate that there is no observable difference in morphology between these two methods. The small particles agglomerated loosely and the particle sizes are *ca.* 8 and 7 nm for the INS and SBS methods, respectively, the latter is slightly lower than the value obtained from XRD data (11 nm, see Table 1).

As a comparison, Table 2 shows the copper contents, the particle size of copper and surface areas of the Cu–ZrO_2 catalysts prepared by the sol–gel method, combined with supercritical drying.[2] Recently, sol–gel chemistry, combined with supercritical drying, has attracted considerable attention for the preparation of supported metal catalysts,[2,29,30] since it produces homogeneous materials of high surface area and of highly dispersed metals on the support. It can be seen from a comparison of our results with Table 2 that finely dispersed

Table 2 Properties of copper–zirconia aerogels calcined at 300 °C in air, from ref. 2

Aerogels[a]	Cu–Zr atomic ratio	Content of copper mol%	SA/ $m^2\ g^{-1}$	d/nm_{copper} XRD
HT-Cu–ZrO_2[b]	0.04	3.8	128	33
HT-Cu–ZrO_2[c]	0.11	10	100	31
HT-Cu–ZrO_2[c]	0.07	6.5	143	28
LT-Cu–ZrO_2[c]	0.15	13	139	_

[a]HT-high temperature supercritical drying of final gel. LT- low temperature supercritical drying of final gel. [b]Two stage sol–gel process, the copper precursor was added after the zirconia precursor was aged for 1 h in solution. [c]One stage sol–gel process, the precursors of copper and zirconium were mixed together before gelation.

surface copper ions and/or CuO nanoclusters would be attached on the surface of zirconia nanoparticles in our SBS method, while relatively large copper particles (33 nm) were obtained in HT-ZrO_2 (two stage). Also, Cu–ZrO_2 nanopowders have high surface areas after calcination at 500 °C and the surface areas increase with increasing copper content because more copper species are attached on the zirconia surface. All these results indicate that the precipitation with TMAOH by the SBS method is a useful method to synthesize catalysts. The advantages result from the action of TMAOH during the reaction. Fokema *et al.*[25] demonstrated that the use of TMAOH as a precipitant prevents the growth of metal oxide particles, leading to high surface area materials after calcination; Reetz *et al.*[21] demonstrated that the TMA^+ ions stabilized metal colloids, due to the protective layer around the metal preventing aggregation of the particles. In our method, which included the preparation of a zirconia support along with copper, these two factors both played a role in the formation of the nanopowders.

These copper oxide–zirconia materials that have undergone calcination at 500 °C are potentially applicable for catalytic processes due to their high surface areas and the high interfacial contact between the zirconia and copper oxide.

Conclusion

Copper oxide–zirconia materials with high surface area and different contents of copper were prepared by precipitation with TMAOH. Using the SBS method, tetragonal zirconia was obtained after calcination at 500 °C in the range of 10–30% copper, indicating that the copper was monodispersely distributed on the surface of the ZrO_2 particles (*ca.* 7 nm). This would be a promising catalyst because of the high surface area and high interfacial contact between ZrO_2 and copper. Using the INS method, tetragonal zirconia was obtained after calcination at 500 °C in the range of 10–15% copper, but the peaks indexed to tetragonal zirconia in the XRD patterns were shifted to higher angle with an increase in copper content, indicating that copper was incorporated in the zirconia lattice. Amorphous composites were obtained at high content of copper (30%). The phase changes with calcination temperature demonstrated that 500 °C was a transition point, while at low (400 °C) or high (700 °C) temperatures tetragonal zirconia with copper oxide was observed from XRD patterns.

Acknowledgements

We gratefully acknowledge Markus Antonietti for support and helpful discussions, Ingrid Zenke for the measurements of wide-angle XRD, and Jurgen Hartmann and Rona Pitschke for their assistance with TEM measurements. The ZEIT-Stiftung and the Max Planck Society are acknowledged for financial assistance.

References

1 G. C. Chinchen, P. J. Denny, J. R. Jennings, M. S. Spencer and K. C. Waugh, *Appl. Catal.*, 1988, **36**, 1–65.
2 R. A. Köppel, C. Stöcker and A. Baiker, *J. Catal.*, 1998, **179**, 515–527.
3 S. Fujita, Y. Kanamori, A. M. Satriyo and N. Takezawa, *Catal. Today*, 1998, **45**, 241–244.
4 Y. W. Suh, S. H. Moon and H. K. Rhee, *Catal. Today*, 2000, **63**, 447–452.
5 J. Sloczynski, T. Bobinska, R. Grabowski, A. Kozlowska, M. Lachowska and J. Skrzypek, *Przem. Chem.*, 2000, **79**, 120.
6 J. P. Breen and J. R. H. Ross, *Catal. Today*, 1999, **51**, 521–533.
7 B. A. Peppley, J. C. Amphlett, L. M. Kearns and R. F. Mann, *Appl. Catal. A*, 1999, **179**, 21–29.
8 Y. Okamoto, H. Gotoh, H. Aritani, T. Tanaka and S. Yoshida, *J. Chem. Soc., Faraday Trans.*, 1997, **93**, 3879–3885.
9 P. G. Harrison, C. Bailey, W. Daniell, D. Zhao, I. K. Ball, D. Goldfarb, N. C. Lloyd and W. Azelee, *Chem. Mater.*, 1999, **11**, 3643–3654.
10 P. G. Harrison, I. K. Ball, W. Azelle, W. Daniell and D. Goldfarb, *Chem. Mater.*, 2000, **12**, 3715–3725.
11 Y. Okamoto and H. Gotoh, *Catal. Today*, 1997, **36**, 71–79.
12 H. Aritani, S. Kawaguchi, T. Yamamoto, T. Tanaka, Y. Okamoto and S. Imamura, *Chem. Lett.*, 2000, **5**, 532–533.
13 G. Centi, G. Cerrato, S. D'Angelo, U. Finardi, E. Giamello, C. Morterra and S. Perathoner, *Catal. Today*, 1996, **27**, 265–270.
14 B. Denise and R. P. A. Sneeden, *Appl. Catal.*, 1986, **28**, 235–239.
15 Y. Amenomiya, *Appl. Catal.*, 1987, **30**, 57–68.
16 I. A. Fisher, H. C. Woo and A. T. Bell, *Catal. Lett.*, 1997, **44**, 11–17.
17 R. A. Köppel, A. Baiker and A. Wokaun, *Appl. Catal.*, 1992, **84**, 77.
18 Y. Nitta, T. Fujimatsu, Y. Okamoto and T. Imanaka, *Catal. Lett.*, 1993, **17**, 157–165.
19 J. Wambach, A. Baiker and A. Wokaun, *Phys. Chem. Chem. Phys.*, 1999, **1**, 5071–5080.
20 T. Munoz, A. M. Prakas, L. Kevan and L. Balkus, *J. Phys. Chem. B*, 1998, **102**, 1379.
21 M. T. Reetz, W. Helbig, S. A. Quaiser, U. Stimmung, N. Breuer and R. Vogel, *Science*, 1995, **267**, 367–269 and references therein.
22 U. Kolb, S. A. Quaiser, M. Winter and M. T. Reetz, *Chem. Mater.*, 1996, **8**, 1889–1894 and references therein.
23 H. Bönnemann, G. Braun, W. Brijoux, R. Brinkmann, A. S. Tilling, K. Seevogel and K. Siepen, *J. Organomet. Chem.*, 1996, **520**, 143–162 and references therein.
24 A. Chemseddine and T. Moritz, *Eur. J. Inorg. Chem.*, 1999, 235–245.
25 M. D. Fokema, E. Chiu and J. Y. Ying, *Langmuir*, 2000, **16**, 3154–3159.
26 H. P. Klug and L. E. Alexander, *X-Ray Diffraction Processes*, Wiley, New York, 1974.
27 G. E. Rush, A. V. Chadwick, I. Kosacki and H. U. Anderson, *J. Phys. Chem. B*, 2000, **104**, 9597–9606.
28 M. Z. Su, *Introduction to Solid Chemistry*, Peking University Press, Beijing, 1987.
29 N. Husing and U. Schubert, *Angew. Chem., Int. Ed.*, 1998, **37**, 22–45.
30 M. Su, B. Zheng and J. Liu, *Chem. Phys. Lett.*, 2000, **322**, 321–326.